

## Cluster-variation–Padé-approximants method and the critical exponents of the fcc Ising model

Alessandro Pelizzola

*Istituto Nazionale di Fisica della Materia and Dipartimento di Fisica del Politecnico di Torino, I-10129 Torino, Italy*

(Received 19 December 1995)

We report results of the application of a recently proposed technique, which combines the cluster variation method (CVM) and Padé approximants, to the analysis of the critical behavior of the face-centered-cubic Ising model. The highest-order CVM approximation ever considered for this lattice is used to estimate magnetization and susceptibility, which are then analyzed by means of Dlog Padé approximants in order to extract information about the critical behavior, taking also into account the effects of confluent singularities. Our results are in good agreement with the most recent simulation and series expansion estimates and require a remarkably small numerical effort. [S1063-651X(96)11805-5]

PACS number(s): 05.50.+q

It is well-known that mean-field approximations and their generalizations are not adequate to describe the critical-point behavior of low-dimensional Ising-like models with short-range interactions, because of the effects associated with the divergence of the correlation length, which cannot be taken into account by approximations dealing with finite clusters and finite numbers of degrees of freedom.

However, Kikuchi [1] developed a variational technique named the cluster variation method (CVM) that was subsequently reformulated by several authors [2], which can describe very accurately the low- and high-temperature behavior of thermodynamical quantities like specific heat, order parameter, response and correlation functions, at such a point that it has been shown by Aggarwal and Tanaka [3] that the method exactly reproduces many terms of the low- and high-temperature series expansions of these quantities. This observation led us to propose a technique [4] for the analysis of critical-point behavior in Ising-like models, which uses Kikuchi's CVM to estimate accurately low- and high-temperature values of quantities that are singular at the critical point, and Padé approximants [5,6] as a tool to extract information about critical-point behavior. This technique will be called the cluster-variation–Padé-approximants method (CVPAM) from now on.

The results of the first test applications of the CVPAM on the Ising model in two and three dimensions were quite encouraging [4], although the largest clusters used were composed of no more than seven to eight points. In a subsequent work, we applied our method to the semi-infinite Ising model in three dimensions [7] using 20-point clusters and obtained results as accurate as those of the most recent Monte Carlo simulations.

In the present paper, we report results for the Ising model on the face-centered-cubic (fcc) lattice, obtained by means of the highest-order CVM approximation ever considered for this lattice, involving 13- and 14-point clusters, and show that the CVPAM is a quite promising method, almost at the level of up-to-date extensive Monte Carlo simulations and series expansions, although much less time consuming.

Let us consider the Ising model with only nearest-neighbor interactions, described by the reduced Hamiltonian

$$\frac{\mathcal{H}}{k_B T} = -K \sum_{\langle ij \rangle} s_i s_j, \quad (1)$$

where  $K$  is the (reduced) interaction strength,  $s_i = \pm 1$  is the  $z$  component of a spin-1/2 operator at the lattice site  $i$ , and the first summation is over nearest neighbors (NN).

The CVM, in its modern formulation [2], is based on the minimization of a free-energy density functional that is obtained by a truncation of the cluster (cumulant) expansion of the corresponding functional appearing in the exact variational formulation of statistical mechanics. The particular approximation we use was proposed by Sanchez and de Fontaine [8] and never actually used, because of its great (at least for the computational tools of that time) complexity. It was named the TF approximation since the largest clusters appearing in the expansion are the 13-point cluster obtained by taking a site and its 12 nearest neighbors and the 14-point fcc unit cell. The remaining relevant clusters are the nine-point cluster (quadruple tetrahedron) obtained by removing a face from the fcc unit cell; the six-point cluster (double tetrahedron, half of the preceding) obtained by removing two adjacent faces from the fcc unit cell; and the four-point single tetrahedron.

For each of these clusters we introduce a density matrix  $\rho_n$ , where  $n$  is the number of sites in the cluster. Notice that, since we are dealing with a classical model, only diagonal elements of such matrices are different from zero.

Using the result by Sanchez and de Fontaine [8] for the exponential of the entropy, the free-energy density functional to be minimized can be written in terms of the density matrices, obtaining

$$\begin{aligned} f(\rho_{13}, \rho_{14}) = & -6K \text{Tr}(s_1 s_2 \rho_4) + \text{Tr}(\rho_{13} \ln \rho_{13}) + \text{Tr}(\rho_{14} \ln \rho_{14}) \\ & - 6\text{Tr}(\rho_9 \ln \rho_9) + 6\text{Tr}(\rho_6 \ln \rho_6) - 2\text{Tr}(\rho_4 \ln \rho_4), \end{aligned} \quad (2)$$

where  $\text{Tr}(s_1 s_2 \rho_4)$  is the NN correlation function ( $s_1$  and  $s_2$  can be any two spins of the single tetrahedron) and only  $\rho_{13}$  and  $\rho_{14}$  are treated as independent variables, since the remaining density matrices can be defined as partial traces of these. For  $\rho_9$  (and then  $\rho_6$  and  $\rho_4$ ) to be properly defined,  $\rho_{13}$  and  $\rho_{14}$  must satisfy the compatibility condition

$$\text{Tr}_{13 \setminus 9} \rho_{13} = \text{Tr}_{14 \setminus 9} \rho_{14}, \quad (3)$$

TABLE I.  $T_c$  estimates for  $b=15$ .

$L$	$[L, L-1]$	$[L, L]$	$[L, L+1]$
8	9.8028	9.7866	9.7953
9	9.8001	9.7956	9.8011
10	9.8015	9.8014	9.8006
11	9.7970	9.8027	9.9059
12	9.8013	9.8017	9.8009
13	9.8007	9.8007	9.8011
14	9.8010	9.8022	9.8011
15	9.8008	9.8006	9.8007
16	9.8007	9.8007	9.8005
17	9.8008	9.8024	9.8014
18	9.8025	9.8011	9.8019
19	9.8010	9.8013	9.8000
20	9.8016	9.8005	9.8010

where  $\text{Tr}_{13\setminus 9}$  denotes a summation over all the spins of the 13-point cluster except those of the nine-point cluster, and similarly for  $\text{Tr}_{14\setminus 9}$ . Finally,  $\rho_{13}$  and  $\rho_{14}$  must also satisfy the normalization condition  $\text{Tr}\rho_{13}=\text{Tr}\rho_{14}=1$ .

In order to reduce our variational problem, which in principle has  $2^{13}+2^{14}$  variables (the diagonal elements of  $\rho_{13}$  and  $\rho_{14}$ ) and  $2^9+1$  linear constraints (one for each diagonal element of  $\rho_9$  and one for the normalization), we can take advantage of the symmetries of the lattice to identify nondegenerate configurations for each cluster, together with their multiplicities, as discussed in detail in Ref. [9] in the case of smaller clusters. Such nondegenerate configurations turn out to be 554 for  $\rho_{14}$ , 288 for  $\rho_{13}$  (corresponding to those determined by Clapp [10] in a different context) and 102 for  $\rho_9$ , thereby reducing our problem to one in 842 variables with 103 linear constraints among them [11]. The latter can now be solved numerically by means of an iterative approach called the natural iteration method [9,12] in a time of the order of the minute (on small workstations) for each value of  $K$  (not too close to  $K_c$ ).

In the CVPAM one calculates a thermodynamical function  $F$ , like the magnetization or the susceptibility, for a set of closely spaced values of a suitable temperaturelike vari-

TABLE II.  $\beta$  estimates from biased approximants for  $T_c=9.801$ .

$L$	$[L, L-1]$	$[L, L]$	$[L, L+1]$
4	0.32150	0.32046	0.32178
5	0.32090	0.32139	0.32135
6	0.32133	0.32135	0.32138
7	0.32136	0.32140	0.32089
8	0.32138	0.32136	0.32134
9	0.32141	0.32178	0.32138
10	0.32139	0.32138	0.32139
11	0.32139	0.32138	0.32137
12	0.32138	0.32138	0.32137
13	0.32138	0.32138	0.32137
14	0.32137	0.32137	0.32137
15	0.32136	0.32136	0.32135

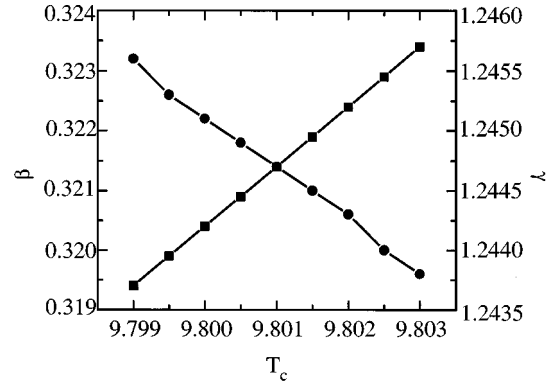


FIG. 1. The critical exponents  $\beta$  (squares, left axis) and  $\gamma$  (circles, right axis) vs the critical temperature  $T_c$  as given by biased Dlog Padé approximants.

able, with a step  $\delta x$  and up to a limiting value  $x_{\max} < x_c$ , where  $x_c$  corresponds to the critical temperature. The  $x_{\max}$  value is chosen, according to the rules outlined in Ref. [4], as the point at which  $F$  differs by  $\epsilon=10^{-5}$  from the result of a simpler approximation, in this case the oriented rhombohedron approximation [9]. This choice ensures that the errors on  $F$  will be of order  $\epsilon$  for the oriented rhombohedron approximation and considerably smaller for the TF approximation. The logarithmic derivative of  $F$  is then determined numerically (here by means of a six-point formula), and interpolated by means of Padé approximants.

We recall [5,6] that an  $[L, M]$  Padé approximant in the variable  $x$  is defined as the ratio of two polynomials of degree  $L$  and  $M$ , respectively:

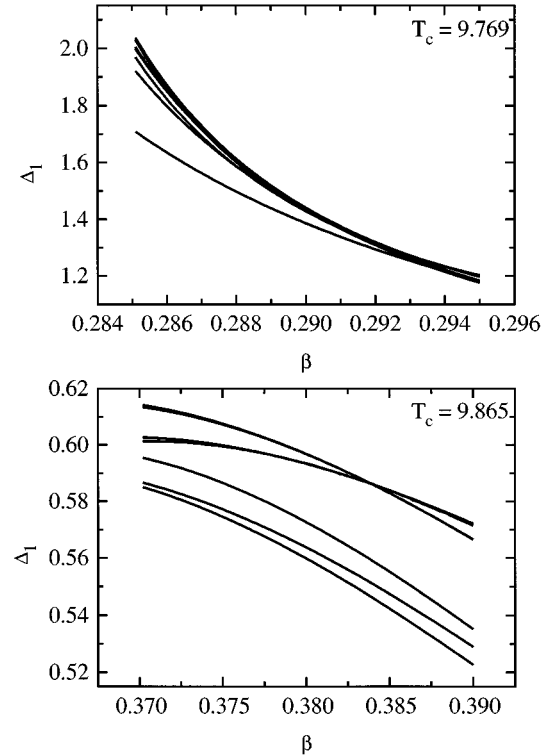


FIG. 2.  $\Delta_1$  vs  $\beta$  plot obtained by method  $M1$  for trial critical temperatures  $T_c=9.769$  and  $9.865$ , respectively, lower and higher than the true  $T_c$ . Data is from the seven  $[L, M]$  approximants with  $6 \leq L+M \leq 10$  and  $|L-M| \leq 1$ .

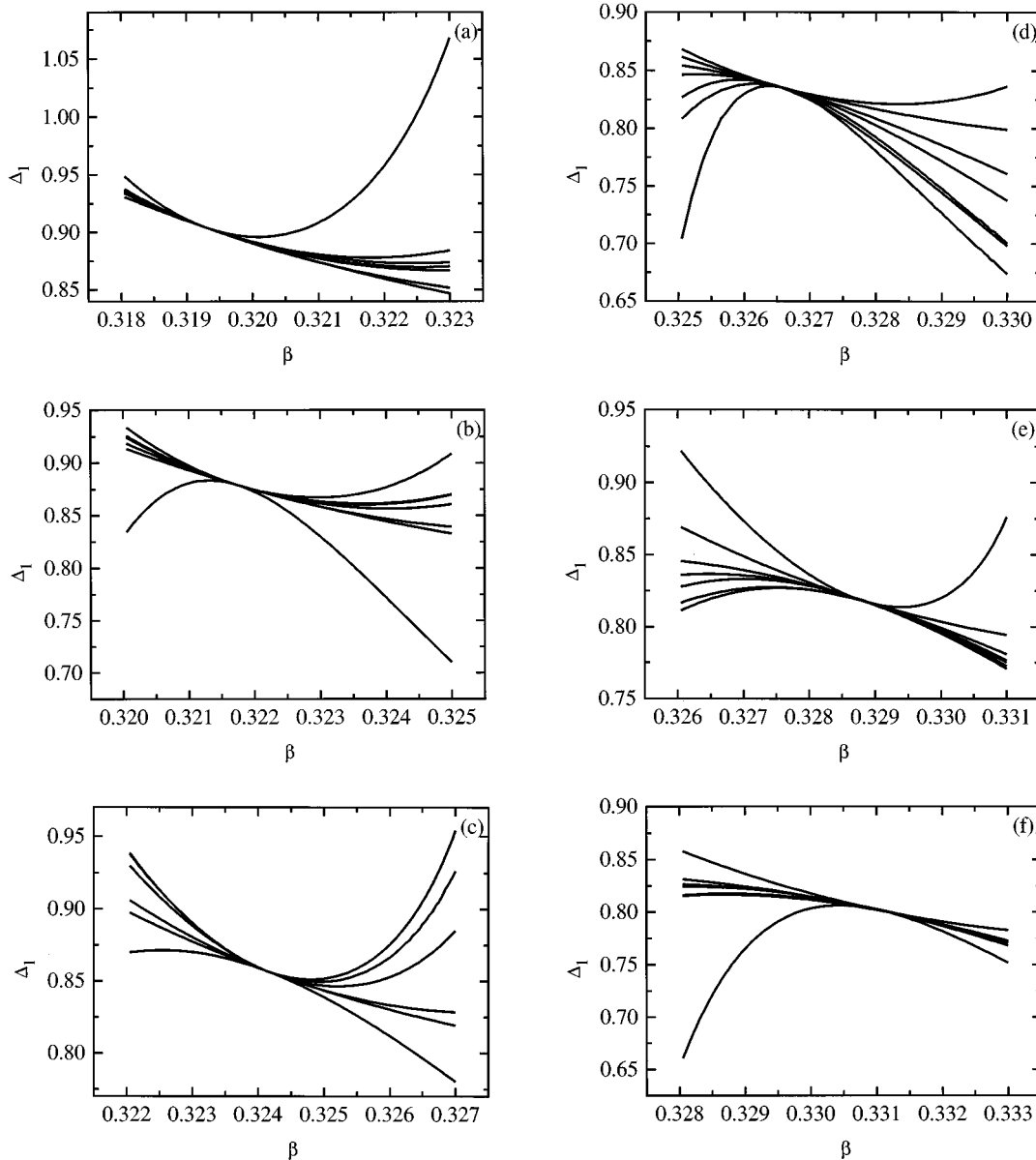


FIG. 3. Confluent exponent  $\Delta_1$  vs  $\beta$ , as given by method M1, for  $T_c = 9.795$  (a), 9.797 (b), 9.799 (c), 9.801 (d), 9.803 (e), and 9.805 (f). The same approximants of Fig. 2 have been used, except for case (c), where the [5,4] approximant has been discarded because it was defective.

$$[L, M](x) \equiv \frac{P_L(x)}{Q_M(x)} \equiv \frac{p_0 + p_1x + p_2x^2 + \dots + p_Lx^L}{q_0 + q_1x + q_2x^2 + \dots + q_Mx^M}, \quad (4)$$

and is generally normalized by setting  $q_0 = 1$  (or  $p_0 = 1$ ). If an  $[L, M]$  Padé approximant is used to approximate the function  $D(x) = (d/dx) \ln F(x)$ , with  $F(x)$  diverging at  $x_c$  as  $(x_c - x)^{-\lambda}$ , then the critical point can be estimated as a pole of  $[L, M](x)$ , and the critical exponent  $\lambda$  as the corresponding residue [5,6]. Since an  $[L, M]$  approximant has  $L + M + 1$  free parameters we must use  $L + M + 1$  interpolation points, given by  $x_n = x_{\max} - n\Delta x$ ,  $n = 0, 1, \dots, L + M$ , where  $\Delta x = b\delta x$  and  $b$  is an integer.

Using the TF approximation, we have calculated the order parameter  $m(z)$  of the fcc Ising model for 800 equally spaced values of  $z = e^{-K}$  (a typical low-temperature expansion variable), with a step  $\delta z = 5 \times 10^{-4}$  and up to the limiting value  $x_{\max} = 0.871$ . On the high-temperature side, the

susceptibility  $\chi(w)$  has been calculated for 600 values of  $w = \tanh K$ , with  $\delta w = 5 \times 10^{-5}$  and up to  $w_{\max} = 0.048$ . All the data have been obtained in about one day of CPU time on a DEC AXP 3000 workstation (significantly lower than the time taken by extensive Monte Carlo simulations or series expansions), while the analysis in the following has been done interactively.

A preliminary analysis with Padé approximants to  $(d/dz) \ln m(z)$  has been carried out to determine the critical point. In Table I we report a set of estimates of  $T_c \equiv 1/K_c$  obtained for  $b = 15$ , from which one could deduce  $T_c = 9.801$ . Values of  $b$  ranging from 10 to 20 yield essentially the same results, although slightly more scattered; almost all entries, however, are in the range 9.799 to 9.803, corresponding to  $0.10166 < w_c < 0.10170$ , which has to be compared with the estimates 0.010172 by Guttman [13] and 0.10175 by Adler [14].

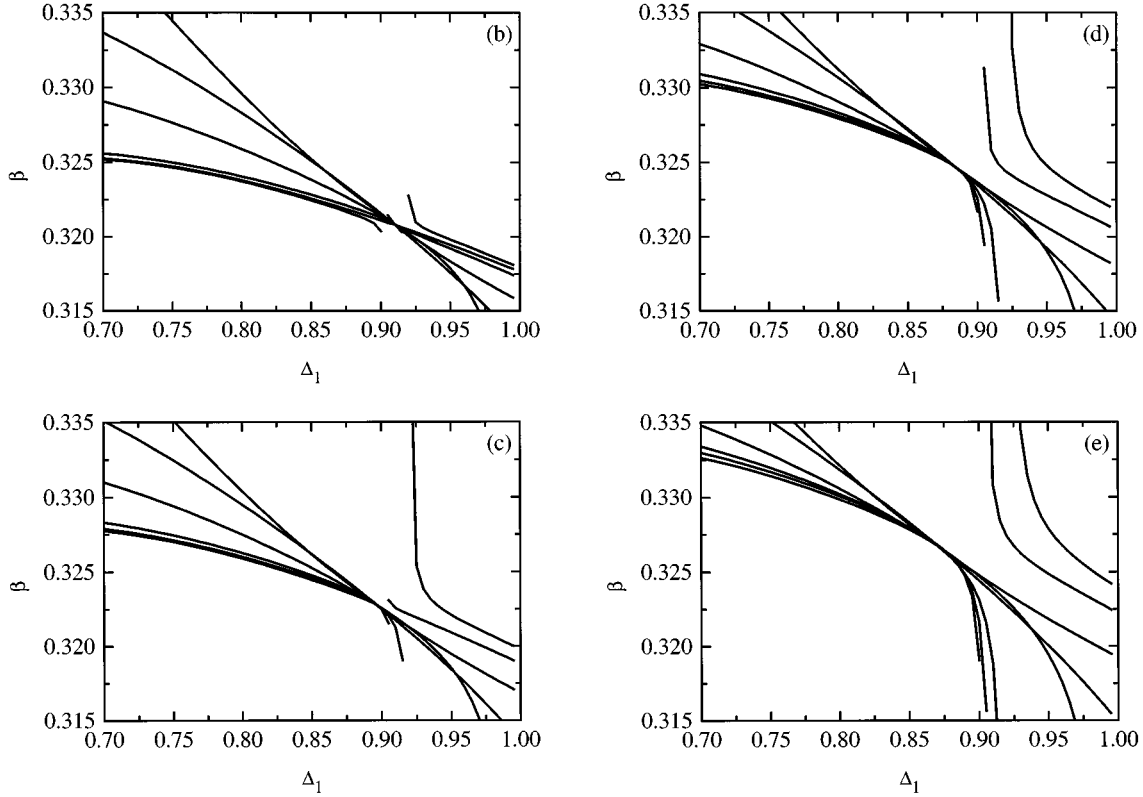


FIG. 4. Critical exponent  $\beta$  vs  $\Delta_1$ , as given by method  $M2$ , for  $T_c = 9.797$  (b),  $9.799$  (c),  $9.801$  (d), and  $9.803$  (e). Data is from the approximants  $[3,2]$ ,  $[3,3]$ ,  $[3,4]$ ,  $[4,3]$ ,  $[4,4]$ , and  $[5,4]$ . There is no sublabel (a) here in order to maintain the correspondence between Figs. 3, 4, and 5.

Using this range of values for the critical temperature, one can easily construct biased approximants [5] for both the magnetization and the susceptibility, by forcing them to be singular at the desired critical point. From now on, we shall always use  $b=15$ , because all the results are essentially unchanged over a wide range of  $b$  values.

The Padé tables produced by biased approximants are very stable (see Table II for an example) and varying  $T_c$  in the range corresponding to our estimate we have obtained the values of  $\beta$  and  $\gamma$  reported in Fig. 1. It can be seen that the values of  $\beta$  (respectively  $\gamma$ ) are slightly lower (respectively higher) than the commonly accepted ones, and at least two possible explanations for this discrepancy must be considered.

As a first attempt, one might try to use the critical temperature estimate by Liu and Fisher (although ours is very close to Guttman's and Adler's),  $w_c \approx 0.10206$ , [15] but this would significantly lower the  $\beta$  estimate ( $0.30 \div 0.31$ ) and raise  $\gamma$  ( $1.26 \div 1.27$ ). It appears that this hypothesis has to be rejected.

Another possibility, which has been proven to be very useful in the past [14,16,17] to remove discrepancies between renormalization-group and high-temperature series expansions results, is to take into account confluent corrections to scaling; that is, to assume that the singularity of  $F(x)$  has the form

$$(x_c - x)^{-\lambda} [1 + a(x_c - x)^{\Delta_1}], \quad (5)$$

by means of the method developed by Adler [14,17,18] for series analysis.

A first method, denoted by  $M1$ , considers Padé approximants to the logarithmic derivative of the function

$$B(x) = \lambda F(x) - (x_c - x) \frac{dF(x)}{dx} \quad (6)$$

instead of  $F(x)$ , for assigned  $x_c$  and  $\lambda$ . The dominant singularity in  $(d/dx) \ln B(x)$  in the case  $\Delta_1 < 1$  (respectively  $\Delta_1 > 1$ ) is a pole at  $x_c$  with residue  $h - \Delta_1$  (respectively  $h - 1$ ).

Another method, denoted by  $M2$ , considers, for assigned  $x_c$  and  $\Delta_1$ , the function

$$G(y) = -\Delta_1 (y - 1) \frac{d}{dy} \ln F(x), \quad y = 1 - \left(1 - \frac{x}{x_c}\right)^{\Delta_1}, \quad (7)$$

which should converge to  $\lambda$  for  $y=1$ .

Applying method  $M1$  to our magnetization data we have obtained  $\Delta_1$  versus  $\beta$  for several fixed values of the trial critical temperature. A first observation, very useful to determine  $T_c$ , is that the plots given by  $M1$  have a different curvature above and below  $T_c$ , as can be clearly seen in Fig. 2. Below  $T_c$  the  $\Delta_1$  versus  $\beta$  plot is bent upward, while above  $T_c$  it is bent downward. This behavior was already observed in Ref. [18] for the exactly solved Baxter-Wu model [19].

The above criterion, applied to the series of plots reported in Fig. 3, allows us to estimate the true critical temperature in the range  $9.797 \leq T_c \leq 9.803$  [cases (b)–(e)], while the value

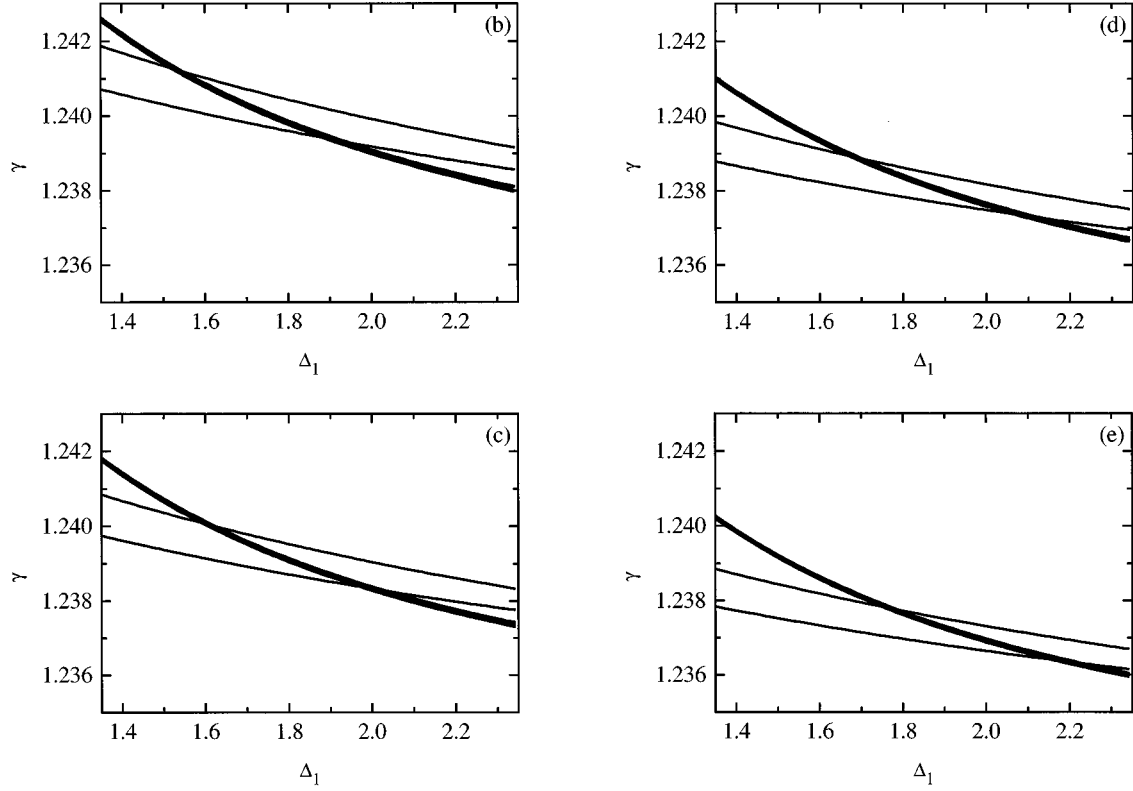


FIG. 5. Critical exponent  $\gamma$  vs  $\Delta_1$ , as given by method  $M2$ , for  $T_c=9.797$  (b), 9.799 (c), 9.801 (d), and 9.803 (e). Data is from  $[L, M]$  approximants with  $3 \leq L \leq 5$  and  $L-1 \leq M \leq L+1$ , except  $[4, 4]$ , which is always defective.

9.795 (respectively 9.805) must certainly be left apart since the corresponding plot is clearly bent upward (respectively downward). Given this range for  $T_c$ , the corresponding estimates for the exponents can be easily deduced from the plots as  $0.321 \leq \beta \leq 0.329$  and  $0.81 \leq \Delta_1 \leq 0.88$ . The result for  $\beta$  represents a remarkable improvement, which indicates that the effect of confluent singularities on critical exponents is not a negligible one, and is then worthy to be considered, although our estimate for the correction to scaling exponent  $\Delta_1$  is significantly higher than the one commonly accepted, which is close to  $1/2$  [14,16,17,20,21] (but Liu and Fisher [15] report that they have obtained results ranging from 0.4 to 0.7).

Method  $M2$  does not appear to provide a clear-cut way to estimate  $T_c$ , so we have retained the result obtained by  $M1$ , and plotted in Fig. 4  $\beta$  vs  $\Delta_1$  for  $T_c$  varying from 9.797 to 9.803. The result for  $\beta$  shrinks to  $0.321 \leq \beta \leq 0.327$ , while the confluent exponent estimate shifts to even higher values,

$0.87 \leq \Delta_1 \leq 0.91$ . One could also try to fix  $\Delta_1$  around  $1/2$ , but this yields very poor results.

The analysis of the susceptibility data is more involved: method  $M1$  does not appear to converge, while method  $M2$  converges only for quite high values of  $\Delta_1$ , around  $1.5 \div 2$ , as can be seen in Fig. 5. Nevertheless, the corresponding  $\gamma$  estimates are very good, being in the range 1.236 to 1.242.

In Table III we have summarized our best estimates and compared them with the most recent results from other methods. The errors quoted for our results are those obtained, as explained above, taking all  $\beta$  and  $\gamma$  estimates from the two Adler methods (for  $\gamma$  only from  $M2$ ) in the range of critical temperatures deduced from the analysis of the  $M1$  results for  $\beta$ . Such error bounds do not, however, account for possible systematic errors introduced by the CVPAM procedure.

It can be seen from Table III that the agreement with the other methods is very good. Taking into account the effects

TABLE III. Recent estimates for the critical exponents  $\beta$  and  $\gamma$ .

Method	$\beta$	$\gamma$
CVPAM (present work)	0.325(4)	1.239(3)
Monte Carlo [22]	0.3258(44)	1.2390(71)
Cluster Monte Carlo [23]	0.319(5)	1.237
Monte Carlo ren. group [24]	0.323(3)	1.241(9)
$\epsilon$ -expansion [25]	0.3270(15)	1.2390(25)
Series expansions [6,26]	0.329(9)	1.243
Series expansions [20]	0.3265(33)	1.237(2)
Coherent-anomaly method [27]	0.327(4)	1.237(4)

of confluent corrections to scaling seems to improve the method, as already happened for series expansions.

As a final remark we notice that the CVPAM method has not reached its limits at all: all the calculations needed for the present paper took about one day of CPU time on a DEC AXP 3000 workstation, and the level of the approximation

can still be improved in several ways on the three cubic lattices, and work is in progress along these lines. Furthermore, all the machinery can be extended in a very straightforward way to models with non-nearest-neighbor or multi-spin couplings, by simply adding linear combinations of the correlation functions to our free-energy density functional.

- 
- [1] R. Kikuchi, Phys. Rev. **81**, 988 (1951).  
 [2] G. An, J. Stat. Phys. **52**, 727 (1988); T. Morita, *ibid.* **59**, 819 (1990).  
 [3] S.K. Aggarwal and T. Tanaka, Phys. Rev. B **16**, 3963 (1977).  
 [4] A. Pelizzola, Phys. Rev. E **49**, R2503 (1994).  
 [5] D.S. Gaunt and A.J. Guttmann, in *Phase Transitions and Critical Phenomena*, edited by C. Domb and M.S. Green (Academic, London, 1974), Vol. 3, and references therein.  
 [6] A.J. Guttmann, in *Phase Transitions and Critical Phenomena*, edited by C. Domb and J.L. Lebowitz (Academic, London, 1989), Vol. 13.  
 [7] A. Pelizzola, J. Magn. Magn. Mat. **140-144**, 1491 (1995).  
 [8] J.M. Sanchez and D. de Fontaine, Phys. Rev. B **17**, 2926 (1978).  
 [9] A. Pelizzola, Physica A **211**, 107 (1994).  
 [10] P.C. Clapp, Phys. Rev. B **4**, 255 (1971).  
 [11] The readers interested in the tables of nondegenerate configurations, multiplicities, and coefficients of the explicit forms of the constraints are invited to contact the author.  
 [12] R. Kikuchi, J. Chem. Phys. **60**, 1071 (1974); **65**, 4545 (1976).  
 [13] See Ref. [6], p. 102; notice also that in Ref. [4] this value is not reported correctly.  
 [14] J. Adler, J. Phys. A **16**, 3585 (1983).  
 [15] A.J. Liu and M.E. Fisher, Physica A **156**, 35 (1989).  
 [16] J. Zinn-Justin, J. Phys. **42**, 783 (1981).  
 [17] J. Adler, M. Moshe, and V. Privman, Phys. Rev. B **26**, 3958 (1982).  
 [18] J. Adler, I. Chang, and S. Shapira, Int. J. Mod. Phys. C **4**, 1007 (1993).  
 [19] R. Baxter and F. Wu, Phys. Rev. Lett. **31**, 1294 (1973).  
 [20] B.G. Nickel and J.J. Rehr, J. Stat. Phys. **61**, 1 (1990).  
 [21] C.F. Baillie *et al.*, Phys. Rev. B **45**, 10438 (1992).  
 [22] A.M. Ferrenberg and D.P. Landau, Phys. Rev. B **44**, 5081 (1991).  
 [23] C. Ruge, P. Zhu, and F. Wagner, Physica A **209**, 431 (1994).  
 [24] H.W.J. Blöte *et al.*, Physica A **161**, 1 (1989); the results quoted here are obtained using scaling laws and their results for the correlation length exponent  $\nu$  and the magnetic exponent  $y_H$ .  
 [25] J.-C. Le Guillou and J. Zinn-Justin, Phys. Rev. B **21**, 3976 (1980); J. Phys. **48**, 19 (1987).  
 [26] A.J. Guttmann and I.G. Enting, J. Phys. A **26**, 807 (1993).  
 [27] M. Kolesik and M. Suzuki, Physica A **215**, 138 (1995).